

# An Experiment to Measure Heat Capacity of $^3\text{He}$ in Aerogel

Jizhong He\*, A.D. Corwin\*, N. Mulders<sup>†</sup>, J.M. Parpia\*,  
J.D. Reppy\*, and M.H.W. Chan<sup>‡</sup>

\* *LASSP, Cornell University, Ithaca, NY 14853-2501*

<sup>†</sup> *Department of Physics and Astronomy, University of Delaware, Newark, DE 19713*

<sup>‡</sup> *Department of Physics, Penn State University, University Park, PA 16802-6300*

*We describe an experiment to measure the heat capacity of  $^3\text{He}$  in aerogel. A new cell improved over the previous design<sup>1</sup> is shown. The aerogel sample is situated inside an epoxy shell which is also the bob of a torsional oscillator.  $^3\text{He}$  entrained in aerogel is cooled through a  $^3\text{He}$  weak thermal link. Data are being taken at temperatures from 10 mK to below 1 mK. We describe a new analysis procedure that determines both the heat capacity of the cell and the thermal conductance of the weak link.*

*PACS numbers: 67.57.Pq, 67.57.Bc*

## 1. INTRODUCTION

The phase transition of bulk liquid  $^3\text{He}$  as an unconventional BCS superfluid has been extensively studied and very well characterized. As a result,  $^3\text{He}$  in aerogel is a great system which to study the influence of impurities on the phase transition.<sup>2-7</sup> Recently we reported some preliminary results of the heat capacity of  $^3\text{He}$  in aerogel.<sup>1</sup> In that report, we showed that there is a heat capacity peak and that it coincides with the onset of the superfluid decoupling, simultaneously measured with a torsional oscillator, at a suppressed  $T_c$ . Since the heat capacity measurement probes directly the thermodynamic state of the  $^3\text{He}$  inside the aerogel, the coincidence strongly suggests that  $^3\text{He}$  in aerogel does undergo a true thermodynamic transition.

However in the previous experiment, due to a short in the cell heater, the heat capacity could not be measured directly without knowing how much heat is applied. An alternative method of temperature drift measurement

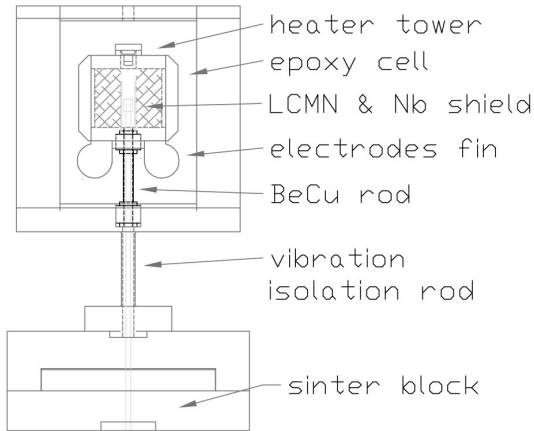


Fig. 1. Schematic drawing of the new cell with the torsional oscillator.

was implemented instead. From the drift measurement, the product of the cell heat capacity  $C$  and the thermal resistance of the weak link between the cell and stage  $R$  was determined. We argued that since there is no known singular feature in the thermal conductivity of the weak link,  $R$  can be treated as a smooth function of  $T$ . Hence the peak like feature in  $RC$  can be regarded as the feature of the heat capacity  $C$ .

In this report, we describe an experiment with a new and improved cell. We show a typical heat pulse taken during our ongoing experiment. We then explain a novel analysis procedure to obtain the heat capacity from the temperature response of the cell temperature.

## 2. APPARATUS

Our new cell design has a similar layout to the old version.<sup>1</sup> The cut-away drawing of the new cell is shown in Fig. 1.  $^3\text{He}$  entrained in the aerogel sample is contained in an epoxy cell shell (Stycast 1266.) The cell is cooled by a silver sinter heat exchanger bolted to a  $\text{PrNi}_5$  nuclear stage plate through a liquid  $^3\text{He}$  weak thermal link. The thermal link is weak enough so that when a heat pulse is applied to the cell, the time it takes for the cell to cool back to the stage temperature is much longer than any other time constant of the cell. This allows the measurement of the cell heat capacity by injecting a known amount of heat into the cell and measuring the temperature response.  $^3\text{He}$  inside the torsion rod and the vibration isolation rod provides the weak thermal link.

The epoxy cell is also the bob of a torsional oscillator of a conventional design.<sup>8</sup> The torsional rod is made of Be-Cu 25. The torsional oscillator allows a simultaneous measurement of the superfluid transition by detecting the viscosity change of liquid  $^3\text{He}$ .

The aerogel sample has a porosity of 97.6%. The sample is a cylinder of 1.2 cm in diameter and 1.3 cm long. In the old cell, the thermometer is located between the cell and the stage and, as a consequence, measures the average temperature of the cell and the stage. In our new cell, we place the LCMN thermometer right in the middle of the aerogel sample. A hole of 0.3 cm in diameter is cut with a special drill into the aerogel. The hole is then fitted with a Nb cylinder to act as a superconductor shield and also to provide trapped static magnetic field of about 2 G. An LCMN salt pill is filled inside a superconducting single coil. An ac SQUID setup, connected to the coil, is used to measure the magnetic flux change in the salt pill as a function of temperature. A melting curve thermometer located at the nuclear stage is used to measure the stage temperature and to calibrate the LCMN thermometer. The cell heater is made of 0.050 mm diameter W-Ti wire, with a 60  $\Omega$  nominal resistance. It is wound tightly around the cylindrical aerogel sample. Another heater, as a backup, is located in a small tower connected to the top of the cell.

### 3. EXPERIMENT AND DATA ANALYSIS

We have an ongoing experiment. During a typical run, the PrNi5 nuclear stage is magnetized to about 7 T and is pre-cooled with a dilution refrigerator to about 8 mK. The stage is then demagnetized to below 1 mK. The cell is cooled down through the weak link, slowly at higher temperatures and faster as the stage is reaching below 1 mK. This is because the thermal resistance and the heat capacity of liquid  $^3\text{He}$  decreases linearly with  $T$ . After the demag, the cell warms up slowly and follows the temperature of the stage. The warming rate is typically slightly faster than  $10\mu\text{K}$  per hour without additional heat input to the stage. The LCMN thermometer is then calibrated against the melting curve thermometer mounted on the stage. Heat pulses are carried out once every half an hour with a duration of about a few minutes and a few nW of power. Fig.2 shows one typical heat pulse response of the cell thermometer. The pressure of the cell is at 22.5 bar.

There are three time constant of interest in the cell. The first is the time constant of the LCMN thermometer, several seconds. It determines the rate of LCMN response at the beginning of the pulse. The short time constant manifests itself as the sharp "foot" in Fig.2. The second time constant is

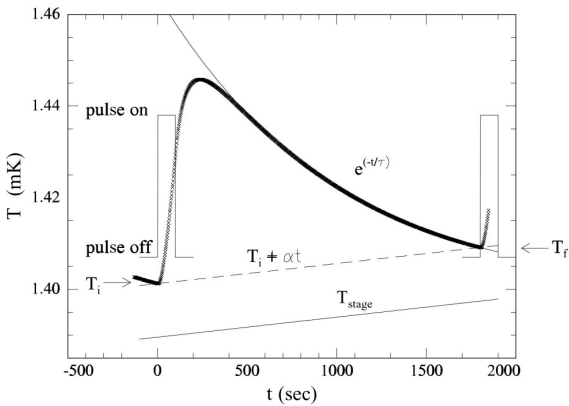


Fig. 2. Temperature response of the cell LCMN thermometer during one of the repeated heat pulses. See the text for detailed explanation.

due to the specific heat of the bulk  $^3\text{He}$  surrounding the LCMN thermometer and the thermal resistance to the  $^3\text{He}$  in the aerogel. It is determined to be about a few minutes. As a result, the LCMN thermometer lags behind the temperature of the cell at the beginning of the pulse. The third and longest time constant, about half of an hour, is due to the relaxation of the cell to the stage temperature. It is the long tail in Fig.2 and is determined by the heat capacity of the cell and the thermal conductance of the weak link.

The heat capacity can be analyzed by solving a set of differential equations and fit the solutions to the data. However, we found a much simpler and more effective way. Since the LCMN thermometer is located right at the top end of the weak link, and the temperature of the lower end is determined by the stage temperature, the heat loss from the cell to the stage through the weak link can be accurately determined, i.e.,

$$Q_{loss} = \int \kappa(T - T_{stage})dt \quad (1)$$

here  $T$  and  $T_{stage}$  are the temperatures of the LCMN thermometer and the stage, and  $\kappa$  is the thermal conductance of the liquid  $^3\text{He}$  column weak link.

The heat capacity is by definition,

$$C = \frac{Q - Q_{loss}}{T - T_i} \quad (2)$$

here  $Q$  is the heat input to the cell, and  $T_i$  is the cell temperature right before the start of the pulse. Treating  $C$  and  $\kappa$  in Eqs.(1,2) as constants in

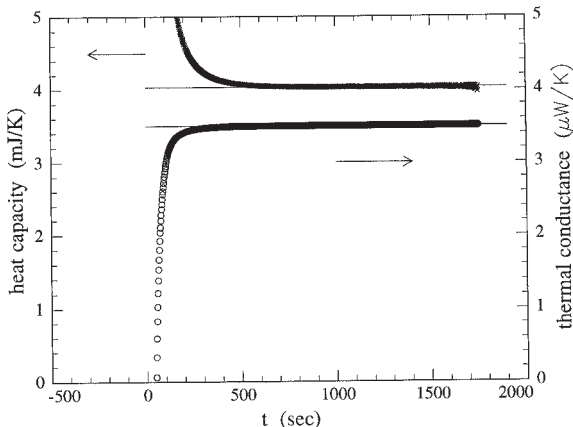


Fig. 3. The heat capacity and thermal conductance results using the analysis described in the text.

the temperature range of interest, they can be solved as:

$$C = \frac{(A_f - A)Q}{A(T - T_i) - A_f(T_f - T_i)} \quad (3)$$

$$\kappa = \frac{(T - T_f)Q}{A(T - T_i) - A_f(T_f - T_i)} \quad (4)$$

where  $A$  is defined as  $\int (T - T_{stage})dt$  and  $T_f$  and  $A_f$  are respectively the temperature and the integral at the end of the pulse. Eqs.(3,4) are valid starting a few minutes after the heat pulse, when the LCMN thermometer tracks the cell temperature. This can be shown in Fig.3 where the temperature response  $T$  in Fig.2 is transformed into  $C$  and  $\kappa$  with Eqs.(3,4). Both  $C$  and  $\kappa$  can be fitted with constants for the later part of the pulse. The residuals of the fits are about the same order as the noise of the data. The goodness of the fits demonstrates the effectiveness of this analysis. As expected, both  $C$  and  $\kappa$  deviates from the constant values at early part of the pulse due to the time constant of the bulk liquid  $^3\text{He}$  surrounding the LCMN thermometer.

#### 4. CONCLUSION

We have described our ongoing experiment to measure the heat capacity of  $^3\text{He}$  in aerogel. We developed a new method of analyzing the heat pulses

to derive the heat capacity of the cell. Additionally, the thermal conductance of the  $^3\text{He}$  thermal link is also measured. With similar measurements done at higher temperatures, it is found that the thermal conductance of the weak links follows a  $1/T$  dependence above 2.3 mK (the  $T_c$  for bulk  $^3\text{He}$  at 22.5 bar):

$$\kappa T = 6.9 \quad (nW) \quad (5)$$

This agrees very well with an estimation,  $\kappa T = 6.7 \quad (nW)$ , based on the geometry and the thermal conductivity value of normal liquid  $^3\text{He}$  at 22.5 bar from Greywall.<sup>9</sup>

This is an ongoing experiment. The main result of the heat capacity of the cell for the whole temperature range will be completed and presented soon.

## ACKNOWLEDGMENTS

We would like to thank Dr. Eric Smith for valuable assistance and discussion during various phases of this work. We would also like to thank Prof. T.L. Ho for useful conversations. This research is funded by NSF under DMR 9705295.

## REFERENCES

1. Jizhong He *et al.*, *J. Low Temp. Phys.* **121**(5/6) 561 (2000)
2. J.V. Porto and J.M. Parpia, *Phys. Rev. Lett.* **74**, 4667 (1995)
3. D.T. Sprague *et al.*, *Phys. Rev. Lett.* **75**, 661 (1995); D. T. Sprague *et al.*, *Phys. Rev. Lett.* **77**, 4568 (1996).
4. B.I. Barker *et al.*, *J. Low Temp. Phys.* **113**, 635 (1998); B. I. Barker *et al.*, *Phys. Rev. Lett.* **85**, 2148 (2000).
5. A. Golov *et al.*, *Phys. Rev. Lett.* **82**, 3492 (1999).
6. H. Alles *et al.*, *Phys. Rev. Lett.* **83**, 1367 (1999)
7. E.V. Thuneberg, S.K. Yip, M. Fogelstrom, and J.A. Sauls, *Phys. Rev. Lett.* **80**, 2861 (1998)
8. *Experimental Techniques in Condensed Matter Physics at Low Temperatures*, R.C. Richardson and E.N. Smith, eds. (Addison-Wesley, Redwood City, 1988)
9. Dennis S. Greywall, *Phys. Rev. B* **29** 4933 (1984)